Journal of Psychiatric Research 156 (2022) 679–689

Contents lists available at ScienceDirect

Journal of Psychiatric Research

journal homepage: www.elsevier.com/locate/jpsychires

Maximum downward slope of sleep slow waves as a potential marker of attention-deficit/hyperactivity disorder clinical phenotypes

Alessio Fasano [a,*,1], Carlo Biancardi [b,**,1], Gabriele Masi [b], Stefania Della Vecchia [b], Paolo Frumento [c], Alberto Mazzoni [a], Egidio Falotico [a], Ugo Faraguna [b,d], Federico Sicca [e]

[a] The BioRobotics Institute, Scuola Superiore Sant'Anna, Pisa, Italy
[b] Department of Developmental Neuroscience, IRCCS Stella Maris Foundation, Pisa, Italy
[c] Department of Political Sciences, University of Pisa, Pisa, Italy
[d] Department of Translational Research and of New Surgical and Medical Technologies, University of Pisa, Pisa, Italy
[e] Child and Adolescent Epilepsy and Clinical Neurophysiology Departmental Unit, USL Centro Toscana, 59100, Prato, Italy

ARTICLE INFO

Keywords:
Attention-deficit/hyperactivity disorder
Sleep
NREM
EEG
Slow waves
Slow wave slope

ABSTRACT

Background: Attention-Deficit/Hyperactivity Disorder (ADHD) is a highly heterogeneous diagnostic category, encompassing several endophenotypes and comorbidities, including sleep problems. However, no predictor of clinical long-term trajectories or comorbidity has yet been established. Sleep EEG has been proposed as a potential tool for evaluating the synaptic strength during development, as well as the cortical thickness, which is presumed to be altered in ADHD. We investigated whether the slope of the Slow Waves (SWs), a microstructural parameter of the sleep EEG, was a potential predictive parameter for psychiatric comorbidities and neuropsychological dimensions in ADHD.

Methods: 70 children (58 m; 8.76 ± 2.77 y) with ADHD who underwent psychiatric and neurologic evaluations and a standard EEG recording during naps were investigated. After sleep EEG analysis, we grouped the extracted SWs in bins of equal amplitude and then measured the associations, through generalized linear regression, between their maximum downward slopes (MDS) and the individual scores obtained from clinical rating scales.

Results: The presence of Multiple Anxiety Disorders was positively associated with MDS of medium amplitude SWs in temporo-posterior left areas. The Child Behavior Checklist scores showed negative associations in the same areas for small SWs. The presence of autistic traits was positively associated with MDS of high amplitude SWs in bilateral anterior and temporal left areas. The WISC-IV Processing Speed Index showed negative associations with MDS of small-to-medium SWs in anterior and temporal right areas, while positive associations in posterior and temporal left areas.

Conclusions: Consistency of association clusters' localization on the scalp suggests that variations in the local MDS, revealing alterations of local synaptic strength and/or in daytime use of certain cortical circuits, could underlie specific neurodevelopmental trajectories resulting in different ADHD clinical phenotypes.

1. Introduction

Attention-Deficit/Hyperactivity Disorder (ADHD) is a neurodevelopmental disorder defined by a persistent pattern of inattention and/or hyperactivity-impulsivity that interferes with functioning or development (American Psychiatric Association, 2013). Despite the worldwide prevalence rate of about 5.3% (Polanczyk et al., 2007), and the well-known executive functioning deficits (Faraone et al., 2015), ADHD remains a heterogeneous diagnostic entity, both from a clinical and a neuropsychological point of view, and has unpredictable and widely different outcomes, including a high risk of psychiatric comorbidities (Franke et al., 2018; O'Neill et al., 2017). These include oppositional defiant and conduct disorders, mood and anxiety disorders, and substance use disorder (Biederman et al., 2008; Donfrancesco et al., 2011; Marangoni et al., 2015). Neurodevelopmental disorders, such as

* Corresponding author. The BioRobotics Institute, Scuola Superiore Sant'Anna, Polo Sant'Anna Valdera, Viale Rinaldo Piaggio, 34, 56025, Pontedera, PI, Italy.
** Corresponding author. Child and Adolescent Neuropsychiatric Unit, Fondazione IRCCS Cà Granda Ospedale Maggiore Policlinico, Via Francesco Sforza, 35, 20122 Milano, MI, Italy.
E-mail addresses: a.fasano@santannapisa.it (A. Fasano), carlo.biancardi@policlinico.mi.it (C. Biancardi).
[1] These authors contributed equally to this work.

https://doi.org/10.1016/j.jpsychires.2022.10.057
Received 30 December 2021; Received in revised form 25 August 2022; Accepted 28 October 2022
Available online 8 November 2022

Abbreviations

AAA = Anxious/Depressed, Aggressive Behavior, Attention Problems
AASM = Academy of Sleep Medicine
ADHD = Attention-Deficit/Hyperactivity Disorder
ASD = Autism Spectrum Disorder
CBCL = Child Behavior Checklist
CPRS-R = Conners' Parent Rating Scale - Revised
CT = Cortical Thickness
DSM = Diagnostic and Statistical Manual of Mental Disorders
ECG = electrocardiogram
EEG = Electroencephalogram
EMG = electromyogram
HD-EEG = High Density - EEG
ICA = independent component analysis
MAD = Multiple Anxiety Disorders
MDS = Maximum Downward Slope
MNEGP = Maximal Negative Peak Amplitude
NREM = Non-Rapid Eye Movement
PSI = Processing Speed Index
SW = Slow Wave
SWA = Slow Wave Activity
WISC-IV = Wechsler Intelligence Scale for Children - Fourth Edition

specific learning disabilities, developmental coordination disorder, intellectual disability, tic disorders, and autism spectrum disorder (ASD) are also common comorbidities (Thapar and Cooper, 2016). Furthermore, ADHD is strongly correlated with Sleep Disorders (Cortese, 2015; Gregory et al., 2017), with a prevalence of up to 70% (Sung et al., 2008), which explains why the most recent research is addressing ADHD as a "24-h disorder" (Becker, 2020), where ADHD fosters the disordered sleep and sleep deprivation may worsen ADHD symptoms. Despite these extremely high comorbidity rates, however, no predictors of clinical long-term trajectories or comorbidity have been established yet (Luo et al., 2019).

Overall, structural imaging studies show that pre-pubertal children with ADHD have a delay in the achievement of peak values of cortical thickness (CT), followed by a steeper and greater reduction during adolescence, particularly in the frontal, parietal and temporal areas (Shaw et al., 2007). Moreover, resting-state functional MRI studies in ADHD have shown a lower connectivity within the Default Mode Network and the fronto-striatal circuits regulating cognitive and motivational loops (Faraone et al., 2015). The concurrence of alterations in CT and brain connectivity, together with the deficits in executive and cognitive functions and the high prevalence of sleep disorders, has been the theoretical basis for the development of a research line investigating the sleep EEG Slow Wave activity (SWA) in ADHD (Scarpelli et al., 2019). Slow waves (SWs) are indeed an established sleep EEG marker of neural plasticity and maturation, as well as of cognition, synaptic strength and sleep quality (Cirelli and Tononi, 2019). They are produced by the joint, synchronized, and oscillating activity of thalamic and cortical neurons during NREM sleep (Steriade et al., 2001; Tononi and Cirelli, 2014). The SWA results, at the scalp level, from the synchronization of the EEG SWs across large neuronal populations and represents the power spectrum in the 0.5–4 Hz range. SWA is directly proportional to SWs' magnitude and incidence over time (Riedner et al., 2007). Since SWs are produced by the synchronized activity of cortical neuronal networks, their amplitudes and slopes are directly related to the underlying synaptic strength (Massimini et al., 2004; Tononi and Cirelli, 2014). Further studies have also shown that, in healthy subjects, the developmental trajectories of the SWA are correlated to those of the CT (Cirelli and Tononi, 2019; Feinberg and Campbell, 2013; Goldstone et al., 2018). In addition, a recent meta-analysis has confirmed that, also in ADHD, the SWA development parallels the course of CT (Biancardi et al., 2021), and some studies have already proven a direct link between SWA development alterations and neuropsychological deficits in ADHD (Furrer et al., 2019; Prehn-Kristensen et al., 2013; Ringli et al., 2013).

However, multiple EEG studies (Esser et al., 2007; Jaramillo et al., 2020; Riedner et al., 2007) have shown that a more detailed approach to the analysis of the SWs is to evaluate their slope, particularly the Maximum Downward Slope (MDS). MDS appeared to be the most direct measure of synaptic strength (Jaramillo et al., 2020), although clinical studies using this parameter are still widely lacking.

In this study, we have investigated whether the MDS of sleep EEG SWs in a sample of children with ADHD were associated with both psychiatric comorbidities and neuropsychological dimensions, with the aim of establishing electrophysiological biomarkers that could help disentangle the heterogeneity of ADHD.

2. Methods and materials

2.1. Subjects

The initial clinical sample consisted of 449 children who had received a diagnosis of ADHD (combined presentation or predominantly hyperactive-impulsive presentation) at the Stella Maris Foundation, from January 1999 to January 2020. The children that underwent, in the same period, both a neuropsychiatric evaluation and a sleep EEG recording were included in the study. Exclusion criteria were instead the presence of epilepsy, known genetic syndromes, moderate or severe prematurity at birth, intellectual disability. Patients were also excluded if they did not reach the NREM3 sleep phase during the EEG recording, or if data on the pharmacologic therapy at the time of the EEG acquisition were unavailable. After this selection process, only 70 children (58 boys and 12 girls aged 3–17 y; mean age 8.76; SD 2.77) were included in the second part of the study.

2.2. Clinical data analysis

Medical records were analyzed to look for psychiatric comorbidities, clinical rating scales, and neuropsychological outcomes of ADHD. The clinical variables revealing psychiatric comorbidities, as described in the DSM-5, were the following: *Language Disorder*, *Specific Learning Disorder*, *Autism Spectrum Disorder* (ASD), *Disruptive-Impulse-Control-Conduct Disorders*, *Bipolar and Depressive Disorders*, *Anxiety Disorders*, namely *Separation Anxiety Disorder*, *Social Anxiety Disorder*, *Panic Disorder* or *Generalized Anxiety Disorders*. Anxiety disorders were further divided into the presence of a single anxiety disorder, or the presence of multiple comorbid anxiety disorders, which we named Multiple Anxiety Disorders (MAD) (Masi et al., 2012). We created a category labeled "*Autistic Traits*", which included the patients who had received the diagnosis of Social (Pragmatic) Communication Disorder or were labeled by clinicians as presenting frank autistic traits but did not receive the diagnosis of ASD. The clinical variables that represented the results of standardized questionnaires derived from the following scales: Child Behavior Checklist for children (CBCL, 52/70 patients) (Achenbach, 2001) and Conners' Parent Rating Scale-Revised (CPRS-R, 47/70 patients) (Conners Multi-Health Systems Inc, 2001). Both questionnaires are widely validated as support tools in the diagnosis of ADHD and its comorbidities (Chang et al., 2016). As for the CBCL/6–18, based on previous works on psychiatric symptoms in ADHD (Biederman et al., 2005), we extracted data from the broad scores, namely "*Internalizing Problems*", "*Externalizing Problems*", "*Total Problems*", and from the syndrome specific scores, namely "*Anxious/Depressed*", "*Withdrawn/Depressed*", "*Somatic*

Complaints", "*Social Problems*", "*Thought Problems*", "*Attention Problems*", "*Rule-Breaking Behavior*", "*Aggressive Behavior*". About CBCL/6–18, the profiles relating to *Emotional Dysregulation*, the *Deficient Emotional Self-Regulation* profile, and the *Dysregulation Profile* were also calculated, starting from the AAA (*Anxious/Depressed*, *Aggressive Behavior*, *Attention Problems*) subscales (Masi et al., 2015). The scores from all the CPRS-R scales were evaluated. We also included the outcomes of the Wechsler Intelligence Scale for Children - Fourth Edition (WISC-IV, 21/70 patients) and covered the following indexes: *Full Scale IQ*, *Verbal Comprehension Index*, *Visual Spatial Index*, *Fluid Reasoning Index*, *Working Memory Index*, and *Processing Speed Index* (PSI).

2.3. Sleep EEG signal processing

Sleep recordings were obtained during daytime naps, through a digital video-EEG-polysomnographic system (Grass Technologies, Rhode Island, United States; Micromed, Mogliano Veneto, Italy) (EEG durations are reported in Table 1). Parents were instructed to partially reduce the sleep of their children to 4–5 h the night before the EEG recording. Polysomnographic measurements included 19 EEG electrodes in a standard 10–20 montage (reference based on average of derivations), deltoid muscle surface electromyogram (EMG), and electrocardiogram (ECG). EEG signals were sampled at 200 Hz. Sleep recordings were scored by a trained scorer according to the American Academy of Sleep Medicine (AASM) standardized criteria (Iber et al., 2007). Alice Sleepwear software was used for manual visual epoch-by-epoch scoring on 30s-long segments of neurologic layout of EEG channels. EEG recordings were analyzed using the EEGLAB toolbox (Delorme and Makeig, 2004) and custom scripts in MATLAB (The MathWorks Inc., Natick, MA) for removing artifacts and non-related neurophysiological activities (e.g., paroxysmal abnormalities). First, the sampled EEG signal was high-pass filtered (cut-off = 0.3 Hz) and band-pass filtered (band = 0.5–40 Hz). Sleep epochs were further filtered through visual inspection to remove persistent gross artifacts. In this phase, each epoch was subdivided into five sub-epochs of 6 s for a finer examination. Subsequently, an independent component analysis (ICA) was performed on filtered sleep data to isolate possible non-cerebral signal sources (e.g., eye blinks or muscle activity) (Delorme et al., 2007). EEG signals (i.e., the SWA) were also classified according to their site predominance on the anterior (Fp2, F4, Fp1, F3), central (C3, C4, Fz, Cz), posterior (P4, O2, P3, O1, Pz, Oz), and temporal (F8, T4, T6, F7, T3, T5) brain regions, and as left-sided, right-sided, or bilateral.

2.4. Computation of slow waves' slope

Sleep SWs were automatically detected for each recording channel by means of a custom script, based on algorithms previously validated (Cucchiara et al., 2020; Riedner et al., 2007). In particular, high-frequency artifacts and background noise were preliminarily removed from each individual signal through a Chebyshev Type II filter (band-pass = 0.5–10 Hz, stopband: 0.1 and 15 Hz) to facilitate detection, while achieving minimal wave shape and amplitude distortion. Positive and negative zero-crossings were identified on the filtered signal, as points where the signal passes the 0 V line from negative values to positive ones, and from positive values to negative ones, respectively. Positive signal deflections present an excessive degree of variability compared to the quite stable negative deflections (Riedner et al., 2007). Therefore, we focused only on detecting negative half-waves. Negative half-waves were defined as negative deflections between two consecutive zero-crossings (Mölle et al., 2002). Furthermore, a slow oscillation was defined as a negative half-wave of at least 125 ms and at most 1 s duration, within NREM2 and NREM3 sleep phases (Massimini et al., 2004). We did not set any arbitrary amplitude threshold for the detection, following the approach of other authors in recent works (Riedner et al., 2007; Cucchiara et al., 2020). We checked the goodness of the half-waves detection through visual inspection. An example is shown in Fig. 1.

We stored several wave parameters already known in literature (Massimini et al., 2004). The maximal negative peak amplitude (MNEGP) for a single half-wave was defined as the maximum negative value among the half-wave's peak amplitudes, considering the existence of multi-peak half-waves. Peaks and troughs were identified as zero-crossings of the signal derivative, filtered with a moving average of 0.025 s window. Maximum Downward Slope (MDS) for each half-wave was computed as the maximum of the signal derivative following the negative zero crossing but preceding the most negative peak (see Fig. 1). We subdivided the sample of detected half-waves showing an absolute MNEGP inferior or equal to 100 μV (being −100 μV roughly the 2.5th percentile of the MNEGP distribution) into ten bins of 10 μV, to assess whether the MDS of SWs of different amplitudes were associated to different clinical traits. In each half-waves' subgroup, we computed the mean of their MDS values, for each participant and each channel. We defined also an MDS phase (MDSP) as the time lag of the MDS point of the wave with respect to the initial zero-crossing, this being the starting point of the half-wave, as illustrated in Fig. 1. The mean value of the MDSP in each half-waves' subgroup was computed for each participant and each channel.

2.5. Statistical analysis

Statistical analyses were conducted in RStudio (RStudio Team, 2020), with the objective of assessing statistical associations between the chosen EEG microstructural measures (i.e., mean MDS) and the

Table 1
Sleep/wake durations. Data of wake and sleep durations ($n = 70$ patients). Nine subjects did not have NREM1 sleep stage, one did not have NREM2 sleep stage, six did not have NREM3 sleep stage. None of the subjects presented REM sleep stage. Min, minutes; NREM, nonrapid eye movement; SEM, standard error of the mean; IQR, inter-quartile range.

	Median (IQR)
Total time in bed [min]	35.90 (17.55)
Waking time [min]	8.50 (18.25)
Complete NREM time [min]	24.90 (8.98)
NREM1 time [min]	1.40 (2.43)
NREM2 time [min]	9.20 (6.65)
NREM3 time [min]	15.40 (11.93)

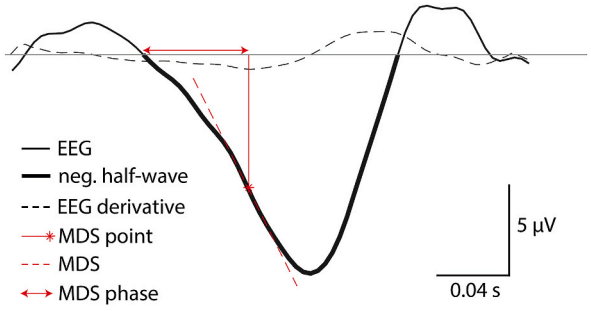

Fig. 1. Slow wave detection and Maximum Downward Slope. Plot of a sleep EEG segment reported in black. A detected half-slow wave is highlighted with a thicker black line. Half-waves were defined as negative deflections between two consecutive zero-crossings. Slow waves were automatically detected using MATLAB script (see the text for details). The signal derivative is the dashed black line. The red, vertical segment with a final red star remarks the wave point where the maximum downward slope (MDS) occurs. The MDS point is defined as the point of maximal derivative of the half-wave signal. The dashed, red line is the tangent to the curve at the MDS point, i.e., the slope. The MDS phase is defined as the time lag between the starting point of the half-wave and the MDS point occurrence (double arrow-segment).

clinical scores, considering the former as independent variables and the latter as dependent variables.

First, we measured associations between the mean MDS in each amplitude bin and the presence/absence of comorbidities with psychiatric and/or neurodevelopmental disorders, via a logistic regression model. We then measured the associations between the EEG variable and the results of the CBCL, CPRS-R, and WISC-IV assessments. For these clinical variables, a linear regression model was employed. Due to the small number of patients with available CBCL 1½-5 questionnaire (n = 6), these variables were not included in the analysis. Age, sex, and psychopharmacotherapy were considered as potential confounders in each model (see Supplementary Material – Table S1 – for a statistical analysis of the influence of these variables on the amplitude of the detected SWs). To minimize the false positives rate, the following non-parametric procedure was devised (Nichols and Holmes, 2002). We randomly generated 2000 rearrangements of the original dependent variable observations. Beta regression coefficients were re-computed at each iteration of the procedure, for each permuted variable. This allowed us to evaluate the sampling distribution of the estimators of regression coefficients under the null hypothesis. The 97.5th and 2.5th percentiles of this distribution were used as critical values for a two-sided test of the estimated coefficients. We evaluated potential clusters of associations on the scalp by selecting only the groups of channels consisting of more than two contiguous electrodes with significant betas (bootstrap-based $p < 0.05$). This threshold was justified by recent results on cluster-size thresholding algorithms implemented elsewhere to correct for multiple comparisons (Bernardi et al., 2015). We further selected only channels presenting significance for at least two consecutive amplitude bins, to consider only consistent associations and to avoid isolated ones, which are likely non-physiological. The same statistical analysis has been conducted on the mean MDSP to find clusters of associations with the clinical scores.

3. Results

3.1. Slow waves amplitudes and slopes

The median MNEGP of the detected SWs, across subjects and channels, was −26.98 μV, with an interquartile range of 26.96 μV. Most of the MNEGP distribution (Fig. 2) laid in the interval (−100, 0 μV), being −100 μV roughly the 2.5th percentile. After the subdivision of this interval in 10 equal bins, we obtained the mean MDS values, which median and interquartile range across all the subjects and channels are reported in Table 2, for each MNEGP bin. Fig. 3 illustrates, as an example, the observed distributions across subjects of the mean MDS for SWs in the absolute MNEGP subgroup (40–50) μV, for each EEG channel.

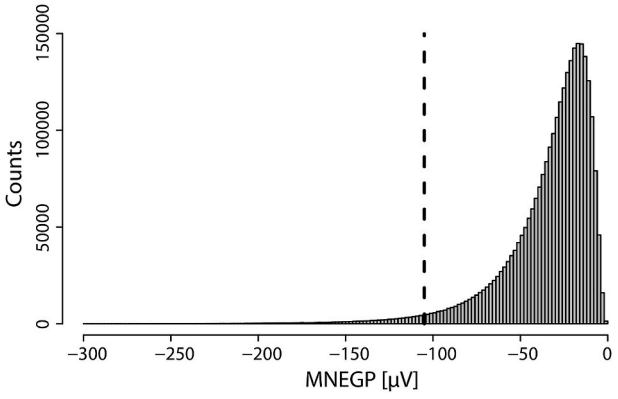

Fig. 2. MNEGP histogram. Distribution of maximum negative peak amplitudes (MNEGP) of detected slow waves for all the participants and all the channels. The dashed line refers to the 2.5th percentile (−104.97 μV). Note that waves with MNEGP lower than −300 μV were cropped.

Table 2
Mean MDS. Median values and interquartile ranges (IQR) of the mean Maximum Downward Slope (MDS), across all subjects and channels, reported for each bin of maximum negative peak amplitudes (MNEGP, reported in absolute values).

MNEGP [μV]	MDS median [μV/s]	MDS IQR [μV/s]
(0–10)	285.64	68.78
(10–20)	425.19	97.94
(20–30)	574.79	107.18
(30–40)	732.23	113.46
(40–50)	888.92	124.93
(50–60)	1044.35	153.56
(60–70)	1189.46	169.95
(70–80)	1333.95	219.29
(80–90)	1485.43	278.05
(90–100)	1620.06	326.49

3.2. Associations MDS-clinical scores

We report in this section the significant cluster of associations between the clinical scores and mean MDS, respecting the prerequisites of consistency across bins and contiguity on the scalp. The topography of these clusters is illustrated in the scalp maps of Figs. 4–6. *P*-values and R^2 for significant associations are reported in Tables 3.1–3.9. Plots of the beta regression coefficients can be found in Supplementary Material (Figs. S1–S28), which also contains the results of the statistical analysis conducted on the mean MDSP (Tab. S2.1-S2.3 for regression values, Figs. S29–S31 for scalp maps of associations). This latter analysis produced significant clusters of associations only for the CPRS-R *ADHD index*, and the CBCL/6–18 scales *"Somatic complaints"* and *"Externalizing problems"*, thus the MDSP resulted less powerful than the MDS as a predictor of comorbidity and neuropsychological profile. We therefore will discuss here only results concerning the MDS.

3.2.1. Comorbidities

With regards to comorbidities (Fig. 4), a positive association was found between comorbid *Multiple Anxiety Disorders* and the mean MDS in channels T5, P3, O1 for MNEGP in (50–60) μV (Tab. 3.1); positive associations between *Autistic Traits* and the mean MDS in channels Fp1, Fp2, F7 for MNEGP in (50–60) μV and in (60–70) μV, in channels Fp1, F7, T3, T5 for MNEGP in (80–90) μV, in channels Fp1, F7, T3 for MNEGP in (90–100) μV (Tab. 3.2).

3.2.2. CBCL/6–18 questionnaires

With regards to the CBCL questionnaires (Fig. 5), negative associations were found between the CBCL/6–18 scale "*Internalizing problems*" and the mean MDS in channels F7, T3, T5 for MNEGP in (0–10) μV, in channels F7, T3, C3, T5, P3 for MNEGP in (10–20) μV, in channels T3, C3, T5, P3, Pz for MNEGP in (20–30) μV, in channels C3, T5, P3, Pz for MNEGP in (30–40) μV (Tab. 3.3); negative associations between the CBCL/6–18 scale "*Withdrawn/depressed*" and the mean MDS in channels T3, T5, P3 for MNEGP in (0–10) μV, in channels C3, T3, T5, P3 for MNEGP in (10–20) μV and in (20–30) μV (Tab. 3.4); negative associations between the CBCL/6–18 scale "*Somatic complaints*" and the mean MDS in channels T3, C3, T5, P3 for MNEGP in (10–20) μV and in (20–30) μV (Tab. 3.5); negative associations between the CBCL/6–18 scale "*Externalizing problems*" and the mean MDS in channels T3, T5, P3, Pz for MNEGP in (10–20) μV and in (20–30) μV (Tab. 3.6); negative associations between the CBCL/6–18 scale "*Aggressive Behavior*" and the mean MDS in channels T3, C3, T5, P3 for MNEGP in (10–20) μV and in (20–30) μV (Tab. 3.7); negative associations between the CBCL/6–18 scale "*Total problems*" and the mean MDS in channels T3, T5, P3, Pz for MNEGP in (10–20) μV and in (20–30) μV (Tab. 3.8).

3.2.3. CPRS-R questionnaires

No significant, consistent clusters of associations were found

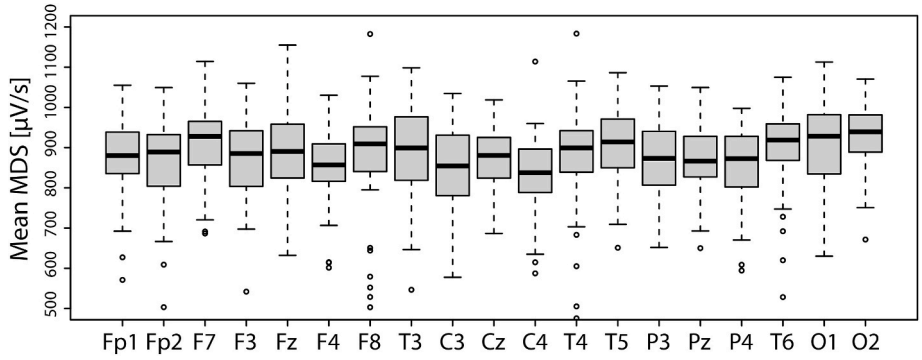

Fig. 3. MDS distributions. Boxplots of distributions across subjects of the mean Maximum Downward Slope (MDS) for the slow waves of Maximum Negative Peak amplitude in the interval (40–50) μV. On the x-axis, corresponding channels of the 10–20 EEG montage are labeled.

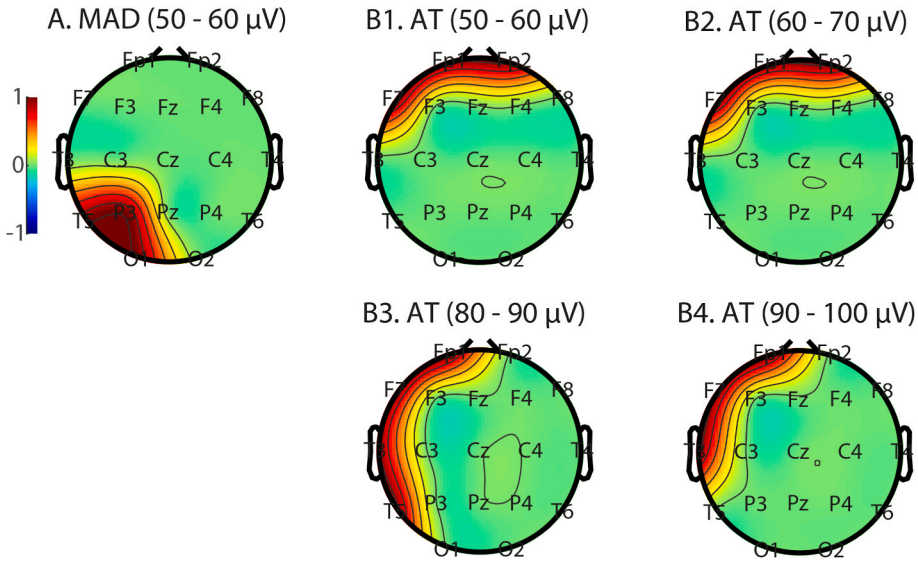

Fig. 4. Associations MDS - comorbidities. Topographical maps of significant association clusters on the representative scalp between the mean Maximum Downward Slope and the presence of clinical comorbidities. Color code refers to the standardized regression betas, rounded to −/+1 and interpolated for visual purposes: red for positive beta, blue for negative beta. **A.** Comorbid Multiple Anxiety Disorders (MAD), in the absolute Maximum Negative Peak (MNEGP) interval (50–60) μV. Significant cluster: T5, P3, O1. **B1.** Comorbid Autistic Traits (AT), in the absolute MNEGP interval (50–60) μV. Significant cluster: Fp1, Fp2, F7. **B2.** Comorbid AT, in the absolute MNEGP interval (60–70) μV. Significant cluster: Fp1, Fp2, F7. **B3.** Comorbid AT, in the absolute MNEGP interval (80–90) μV. Significant cluster: Fp1, F7, T3, T5. **B4.** Comorbid AT, in the absolute MNEGP interval (90–100) μV. Significant cluster: Fp1, F7, T3.

between CPRS-R questionnaires and the mean MDS.

3.2.4. *WISC-IV assessment*

The WISC-IV assessment (Fig. 6) showed negative associations between the *Processing Speed Index* and the mean MDS in channels F4, F8, C4, T4 for MNEGP in (0–10) μV, in channels Fp2, F4, F8, C4, T4, T6 for MNEGP in (10–20) μV and in (20–30) μV; positive associations between the *Processing Speed Index* and the mean MDS in channels C3, T5, P3 for MNEGP in (30–40) μV and in (40–50) μV (Tab. 3.9).

4. Discussion

Our working hypothesis was that a particular feature of the sleep EEG microstructure, namely the SWs' slope, might represent a potential biomarker of psychiatric comorbidities and neuropsychological dimensions in children with ADHD. To explore this hypothesis, we have extracted the SWs' features from a sample of 70 ADHD children. They displayed a male/female ratio and a comorbidity rate equivalent to those of recent literature (Banaschewski et al., 2018). We analyzed the standard EEG recordings during daytime naps after partial sleep deprivation and measured associations between the SWs' mean MDS and a set of standard clinical scores via generalized linear regression models, including age, sex, and psychopharmacotherapy as potential confounders.

The EEG signal analysis presented here suggests that children with ADHD and Multiple Anxiety Disorders (MAD) display greater synaptic strength in the left temporal and posterior areas (see Fig. 4). We also found potential indicators of greater synaptic strength in the anterior areas bilaterally and left fronto-temporal areas in children with ADHD and autistic traits (see Fig. 4). Moreover, we found potential indicators of weaker synaptic strength in central and posterior left areas in children with ADHD and higher CBCL/6–18 scores in the broad scores, and specifically in the subscales addressing depressive symptoms, somatic complaints and aggressive behaviors (see Fig. 5). Finally, we found potential indicators of weaker synaptic strength in anterior and temporal right areas, and stronger synaptic strength in left central and temporo-posterior areas, in children with ADHD and higher Processing Speed Index scores (see Fig. 6). The CPRS-R questionnaires did not produce significant associations on the scalp.

We decided to divide the SWs into distinct amplitude bins because different SWs' amplitudes may underlie different electrophysiological activities. Jaramillo and colleagues (Jaramillo et al., 2020) have recently observed topographic variations with amplitude in the extent of SWs' slope reduction during NREM night sleep of healthy subjects, plausibly indicating amplitude-dependent differences in the generation of SWs. The amplitude of a SW is determined by the synchronization rate of the underlying cortical neurons, namely by the amount of neurons that, in a specific area, are firing at the same time (Esser et al., 2007; Riedner et al., 2007; Vyazovskiy et al., 2007). Steep and high-amplitude SWs reflect an efficient neuronal synchronization that allows for a fast recruitment of a large number of neurons. In contrast, small SWs might reflect local events of tiny groups of neurons. In fact, large groups of

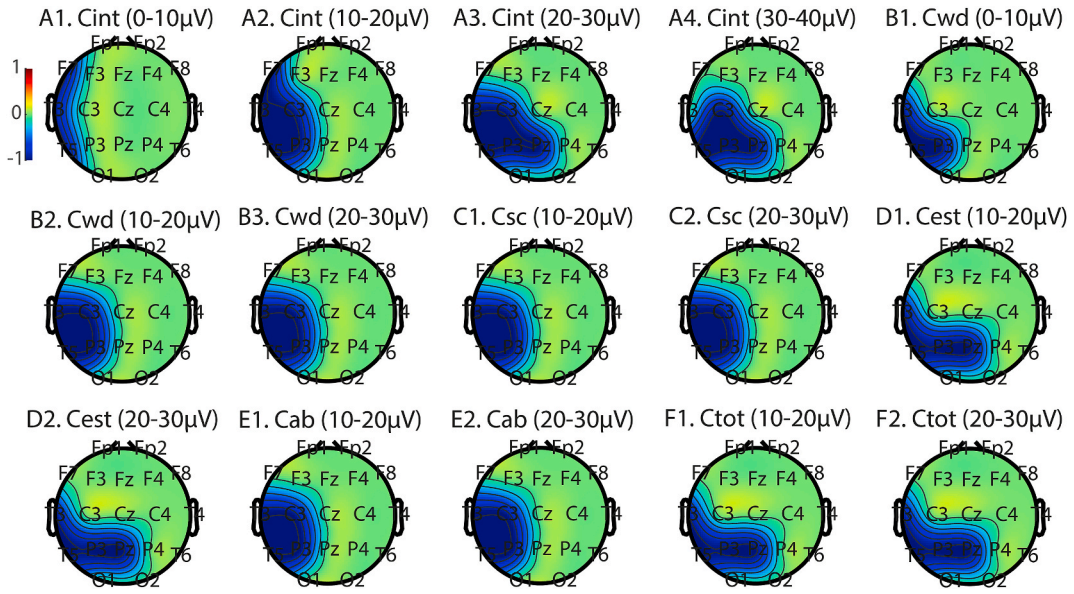

Fig. 5. Associations MDS - CBCL/6–18. Topographical maps of significant association clusters on the representative scalp between the mean Maximum Downward Slope and the scores at the Child Behavior Checklist (CBCL/6–18). Color code refers to the standardized regression betas, rounded to −/+1 and interpolated for visual purposes: red for positive beta, blue for negative beta. **A1.** CBCL/6–18 scale "*Internalizing problems*" (Cint), in the absolute Maximum Negative Peak (MNEGP) interval (0–10) μV. Significant cluster: F7, T3, T5. **A2.** Cint, in the absolute MNEGP interval (10–20) μV. Significant cluster: F7, T3, C3, T5, P3. **A3.** Cint, in the absolute MNEGP interval (20–30) μV. Significant cluster: T3, C3, T5, P3, Pz. **A4.** Cint, in the absolute MNEGP interval (30–40) μV. Significant cluster: C3, T5, P3, Pz. **B1.** CBCL/6–18 scale "*Withdrawn/depressed*" (Cwd), in the absolute MNEGP interval (0–10) μV. Significant cluster: T3, T5, P3. **B2.** Cwd, in the absolute MNEGP interval (10–20) μV. Significant cluster: T3, C3, T5, P3. **B3.** Cwd, in the absolute MNEGP interval (20–30) μV. Significant cluster: T3, C3, T5, P3. **C1.** CBCL/6–18 scale "*Somatic complaints*" (Csc), in the absolute MNEGP interval (10–20) μV. Significant cluster: T3, C3, T5, P3. **C2.** Csc, in the absolute MNEGP interval (20–30) μV. Significant cluster: T3, C3, T5, P3. **D1.** CBCL/6–18 scale "*Externalizing problems*" (Cest), in the absolute MNEGP interval (10–20) μV. Significant cluster: T3, T5, P3, Pz. **D2.** Cest, in the absolute MNEGP interval (20–30) μV. Significant cluster: T3, T5, P3, Pz. **E1.** CBCL/6–18 scale "*Aggressive Behavior*" (Cab), in the absolute MNEGP interval (10–20) μV. Significant cluster: T3, C3, T5, P3. **E2.** Cab, in the absolute MNEGP interval (20–30) μV. Significant cluster: T3, C3, T5, P3. **F1.** CBCL/6–18 scale "*Total problems*" (Ctot), in the absolute MNEGP interval (10–20) μV. Significant cluster: T3, T5, P3, Pz. **F2.** Ctot, in the absolute MNEGP interval (20–30) μV. Significant cluster: T3, T5, P3, Pz.

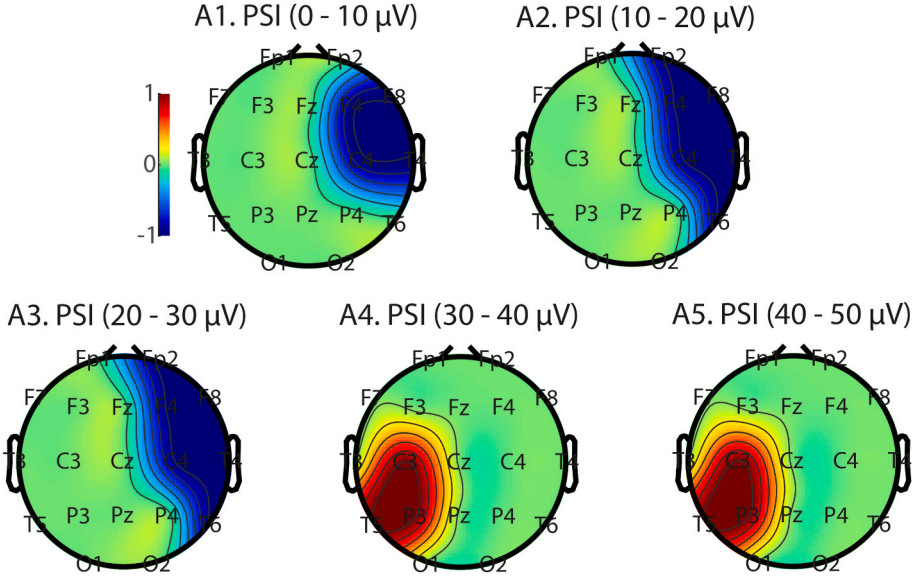

Fig. 6. Associations MDS - WISC—IV. Topographical maps of significant association clusters on the representative scalp between the mean Maximum Downward Slope and the scores at the Wechsler Intelligence Scale for Children – Fourth Edition (WISC—IV). Color code refers to the standardized regression betas, rounded to −/+1 and interpolated for visual purposes: red for positive beta, blue for negative beta. **A1.** WISC—IV scale "*Processing Speed Index*" (PSI), in the absolute Maximum Negative Peak (MNEGP) interval (0–10) μV. Significant cluster: F4, F8, C4, T4. **A2.** PSI, in the absolute MNEGP interval (10–20) μV. Significant cluster: Fp2, F4, F8, C4, T4, T6. **A3.** PSI, in the absolute MNEGP interval (20–30) μV. Significant cluster: Fp2, F4, F8, C4, T4, T6. **A4.** PSI, in the absolute MNEGP interval (30–40) μV. Significant cluster: C3, T5, P3. **A5.** PSI, in the absolute MNEGP interval (40–50) μV. Significant cluster: C3, T5, P3.

neurons will produce high-amplitude SWs even if not strongly connected, while small groups of neurons, even if strongly bound by synaptic connections, will produce low-amplitude SWs. For instance, high-amplitude SWs during NREM2 sleep may also be the so-called "K-complexes". Differently from SWs of intrinsic cortical origin, however, K-complexes are less indicative of the synaptic strength of cortico-cortical connections (Riedner et al., 2007). By analyzing the MDS subdivided into bins of different amplitudes, we have therefore applied a strategy for estimating the synaptic strength of synchronized neurons, relatively less dependent on the sizes of the neuronal circuits generating the SW under examination. The presence of psychiatric comorbidities, namely MAD and Autistic Traits, was associated with MDS of SWs covering the higher portion of our experimental range of absolute amplitudes, i.e., plausibly produced by larger neuronal circuits.

Table 3
Regression R^2. Regression R^2 values for the significant associations (bootstrap-based $p < 0.05$) between the variable of clinical scores and mean Maximum Downward Slope (MDS), for slow waves' Maximum Negative Peak amplitude (MNEGP) subdivided into ten bins (absolute values). McFadden pseudo-R^2 was computed for binary variables, i.e., *Comorbid Multiple Anxiety Disorders*, *Autistic Traits*. In parentheses, we report the sign of the association betas. Bootstrap-based *p*-values, defined as the area under the curve of the permutation distribution of the statistics (Hanley and McNeil, 1982), by asterisk notation: * = $p < 0.05$, ** = $p < 0.01$, *** = $p < 0.001$. Channels on rows are separated by double lines in anterior, temporal, and posterior areas, from the left to the right hemisphere. Note that, in total, we computed 190 *p*-values per each clinical variable. Of those, 5% are expected to be less than 0.05 by sheer chance. If one wanted to apply Bonferroni correction, each *p*-value should be compared with a reference value of $0.05/190 \approx 0.00026$.

Table 3.1 Regression R^2. *Comorbid Multiple Anxiety Disorders*.

		MNEGP [μV]
		(50–60)
Channels	T5	0.42 (+) **
	P3	0.24 (+) **
	O1	0.26 (+) *

Table 3.2 Regression R^2. *Autistic Traits*.

		MNEGP [μV]			
		(50–60)	(60–70)	(80–90)	(90–100)
	Fp1	0.31 (+) **	0.26 (+) *	0.34 (+) **	0.33 (+) **
	Fp2	0.35 (+) **	0.30 (+) **		
Channels	F7	0.32 (+) **	0.33 (+) ***	0.46 (+) ***	0.25 (+) *
	T3			0.41 (+) **	0.28 (+) **
	T5			0.31 (+) **	

Table 3.3 Regression R^2. *CBCL/6–18 scale "Internalizing problems"*.

		MNEGP [μV]			
		(0–10)	(10–20)	(20–30)	(30–40)
	C3		0.17 (−) **	0.16 (−) **	0.12 (−) *
	F7	0.10 (−) *	0.18 (−) **		
	T3	0.17 (−) **	0.23 (−) ***	0.24 (−) ***	
Channels	T5	0.20 (−) **	0.23 (−) ***	0.23 (−) ***	0.17 (−) **
	P3		0.20 (−) ***	0.19 (−) **	0.18 (−) **
	Pz			0.13 (−) *	0.12 (−) *

Table 3.4 Regression R^2. *CBCL/6–18 scale "Withdrawn/depressed"*.

		MNEGP [μV]		
		(0–10)	(10–20)	(20–30)
	C3		0.13 (−) **	0.11 (−) *
	T3	0.15 (−) **	0.20 (−) **	0.20 (−) **
Channels	T5	0.21 (−) **	0.18 (−) ***	0.23 (−) ***
	P3	0.11 (−) *	0.15 (−) **	0.14 (−) **

Table 3.5 Regression R^2. *CBCL/6–18 scale "Somatic complaints"*.

		MNEGP [μV]	
		(10–20)	(20–30)
	C3	0.27 (−) *	0.26 (−) *
	T3	0.28 (−) **	0.26 (−) *
Channels	T5	0.29 (−) **	0.30 (−) **
	P3	0.28 (−) *	0.26 (−) *

Table 3.6 Regression R^2. *CBCL/6–18 scale "Externalizing problems"*.

		MNEGP [μV]	
		(10–20)	(20–30)
	T3	0.14 (−) *	0.24 (−) *
Channels	T5	0.17 (−) **	0.23 (−) *
	P3	0.18 (−) **	0.19 (−) *
	Pz	0.19 (−) **	0.13 (−) *

Table 3.7 Regression R^2. *CBCL/6–18 scale "Aggressive Behavior"*.

		MNEGP [μV]	
		(10–20)	(20–30)
	C3	0.15 (−) *	0.15 (−) *
	T3	0.14 (−) *	0.16 (−) *
Channels	T5	0.17 (−) **	0.16 (−) *
	P3	0.17 (−) **	0.15 (−) *

Table 3.8 Regression R^2. *CBCL/6–18 scale "Total problems"*.

	MNEGP [μV]

(*continued on next page*)

Table 3 (*continued*)

Table 3.8 Regression R^2. *CBCL/6–18 scale "Total problems".*

		MNEGP [μV]	
		(10–20)	(20–30)
Channels	T3	0.16 (−) **	0.18 (−) **
	T5	0.18 (−) **	0.17 (−) **
	P3	0.16 (−) **	0.16 (−) *
	Pz	0.14 (−) *	0.14 (−) *

Table 3.9 Regression R^2. *WISC−IV scale "Processing Speed Index".*

		MNEGP [μV]				
		(0–10)	(10–20)	(20–30)	(30–40)	(40–50)
	C3				0.37 (+) *	0.38 (+) **
	Fp2		0.32 (−) *	0.36 (−) *		
	F4	0.43 (−) **	0.55 (−) ***	0.67 (−) ***		
	C4	0.54 (−) ***	0.54 (−) ***	0.42 (−) **		
Channels	T5				0.40 (+) *	0.34 (+) *
	F8	0.43 (−) **	0.42 (−) **	0.39 (−) **		
	T4	0.33 (−) *	0.45 (−) **	0.38 (−) **		
	T6		0.42 (−) **	0.34 (−) **		
	P3				0.44 (+) *	0.52 (+) **

Instead, the CBCL/6–18 and WISC-IV scores were associated with MDS of lower amplitude SWs, i.e., plausibly produced by smaller neuronal circuits. Furthermore, in this paper, unlike others focusing only on large synchronized global slow waves (Massimini et al., 2004), we did not set any arbitrary amplitude threshold for slow waves detection. This decision finds at least two grounds: i) thresholds set in adults could not be automatically applied to our sample of children; ii) local events would be neglected as their underlying electrophysiological processes possibly groups in two different clusters (type I and type II waves as described in (Siclari et al., 2014; Spiess et al., 2018).

The causality link between these sleep EEG findings and the clinical features is difficult to establish. These results could indicate that a certain decrease or increase in synaptic strength in a given cortical area, respectively featured as a reduction or increase in the MDS, might underlie specific clinical or neuropsychological dysfunction of ADHD. Alternatively, higher or lower MDS in certain brain areas may reflect an increased or reduced use of those areas during the day, as a consequence of the clinical and neuropsychological specificities that characterize the ADHD condition in children. Indeed, the massive use of a brain area during the day results in a greater amount and amplitude of sleep SWs in that area, especially in the first cycles and under sleep deprivation (Ferrarelli et al., 2019; Plante et al., 2016). These different interpretations are not in opposition and could in fact reinforce each other. Taking MAD as an example, our results show a positive association with MDS in the left temporal and posterior areas for SWs of medium amplitude (50–60 μV). ADHD children with MAD might have a greater synaptic strength for medium-sized cortical circuits in those areas and/or they may overuse those circuits during the day, resulting in an increase in SWs' activity and slope at night. Circuits with stronger synaptic connections, however, may themselves represent more susceptible areas for recruitment in brain processing of cognitive and behavioral functions, therefore further fostering synaptic strength through a mutually enhancing circle. Some authors (Almeida Montes et al., 2013) have also hypothesized that the increased synaptic density seen in the posterior brain areas of ADHD children may reflect a compensatory increased use of those areas, in order to overpower the reduced synaptic density in the prefrontal areas underlying the functional deficits.

Moreover, the presence of *Autistic Traits* in our ADHD cohort was positively associated with the MDS in clusters of bilateral anterior electrodes and left fronto-temporal areas. Importantly, these associations interested SWs of higher amplitudes (50–100 μV), i.e., larger neuronal circuits, with respect to the other neuropsychiatric dimensions. It is well known that the developmental trajectories of the SWA in neurotypical children follow the antero-posterior axis, and is strictly correlated to CT development (Cirelli and Tononi, 2019; Feinberg and Campbell, 2013; Goldstone et al., 2018).

It is also well known that children with ADHD show a delay in the achievement of peak values of cortical thickness (CT) (Shaw et al., 2007), and that the consequence of this is a delay in the process of SWA maturation over the antero-posterior axis. This fact has been confirmed by Ringli and coworkers (Ringli et al., 2013), who proved a relative increase in SWA distribution over the central areas in ADHD children, when compared to healthy controls, who, instead, show a relative increase in SWA distribution over the frontal areas. In contrast, ASD children have shown an excess of SWA in prefrontal and frontal areas, compared to neurotypical children (Fauzan and Amran, 2015). A possible interpretation of our finding could therefore be that the ADHD patient with autistic traits ranks intermediate between the sole ADHD and the ASD conditions, with regards to SWA and synaptic density in anterior areas, and this could explain the positive association between the presence of autistic traits and the MDS in clusters of bilateral anterior electrodes and left fronto-temporal areas. A relative overuse of large circuits in antero-temporal areas might also be a distinctive feature of ADHD patients with autistic traits, helping them compensate for their pragmatic deficits that accompany the analysis of social inputs. A future confrontation with neurotypical children could be of great use in investigating this interpretation.

Significant clusters of negative associations between the MDS and the CBCL/6–18 broad score "*Internalizing Problems*" moved from electrodes covering the left temporal areas to electrodes in left central, left temporo-posterior, and midline posterior areas for increasing absolute MNEGP in (0–40 μV). When looking, in particular, at the syndrome subscales "*Withdrawn/Depressed*" and "*Somatic Complaints*", significant negative associations were consistently observed with low amplitude SWs' slopes in the cluster of channels T3, T5, C3, P3. Interestingly, some studies (Armitage et al., 2001, 2002) have shown a lower sleep delta power and functional connectivity in youth with MDD. Same associations on the scalp (T3, T5, C3, P3) for the same SWs' amplitude interval (10–30 μV) were obtained for the CBCL/6–18 subscale "*Aggressive Behavior*", among the "*Externalizing Problems*". Then, both the broad scores "*Externalizing Problems*" and "*Total problems*" were significantly and negatively associated with the MDS of SWs of amplitude range (10–30 μV) from a specific cluster of temporal and posterior electrodes (T3, T5, P3, Pz). Therefore, a weaker MDS in sleep EEG, signaling weaker synaptic strengths and/or daytime underuse of small (i.e., low

amplitude SW-generating) cortical circuits in left temporal and posterior areas, may inform of specific ADHD profiles characterized by worse psychological symptoms, especially psychosomatic and depressive ones, as well as behavioral issues emerging from the CBCL/6–18 questionnaire.

Unexpectedly, we found no significant associations between the CPRS-R scores and the mean MDS. This lack of association might be due to a relative clinical homogeneity of our sample of patients, all sharing a diagnosis of ADHD. Future studies comparing ADHD children with healthy control groups will help further investigate this feature.

Further remarkable results concerned a significant negative association between the *Processing Speed Index* and the MDS (0–30 μV) in a large cluster of anterior and temporal right areas, and a positive association between the same score and the MDS (30–50 μV) for a small cluster of left central and temporo-posterior electrodes. These results suggest that PSI scores might be linked with increased or reduced synaptic strength and/or daytime overuse or underuse of small-to-medium cortical circuits in left or right cortical areas, respectively. Deficits in WISC-IV PSI have been shown to be highly specific for ADHD, even when compared to other psychiatric diseases (Martiny et al., 2020; Walg et al., 2017), and to be predictive of social failure during adolescence (Thorsen et al., 2018). The strong lateralized association of brain connectivity and PSI seen in our ADHD sample may therefore represent a possible biomarker for a neurophysiological-based approach to disease prognosis.

Possible limitations of this work are the following. First, our EEG analysis was based on an average of 24.89 ± 0.78 min of sleep recording because of limitations pertaining to the nature of the sample. A full-night analysis might differentiate between the sleep deprivation effect on the first cycles of sleep and the effect of the underlying neurodevelopment. However, every patient underwent the same acute sleep deprivation. Second, our study was retrospective and thus carries all the flaws of this study design. To tackle this issue, we used strict inclusion criteria to collect samples as homogeneous as possible, and excluded all the patients that had insufficient clinical data. Third, we did not get the data from High Density – EEG (HD-EEG) recordings and analyses, therefore our cluster resolution was ultimately low. However, to limit false positives, we performed a cluster analysis of 3 or more adjacent electrodes, extracting results from relatively wide areas of the cortex. Further HD-EEG investigations will help confirm or possibly refine our results, such as providing a more detailed outline on the scalp of the specific associations with differential aspects of the CBCL syndrome scales. This might be integrated with a finer analysis of the slope at low amplitudes.

Taken together, our results put forward the idea that variations in the local MDS, revealing alterations of local synaptic strength and/or in daytime use of certain cortical circuits, could underlie specific neurodevelopmental trajectories resulting in different clinical phenotypes of ADHD. Furthermore, as associations were amplitude-specific, circuits of different sizes involved in the production of sleep SWs might bring different information about the associated clinical profiles and hence constitute distinct markers. The analysis of the SWs' slope, through sleep EEG, can therefore be an adjunctive parameter for research in ADHD, and a promising and very detailed prognostic tool, especially for featuring the large number of different endophenotypes, comorbidities, and neuropsychological profiles characterizing this disorder (Banaschewski et al., 2018). Although these electrophysiological findings cannot yet address specific therapeutic strategies, the emergence of new treatments, such as the neurofeedback techniques that modulate the electroencephalographic waves, may represent an important resource for obtaining innovative, non-pharmacological, precision medicine interventions, that can at least be part of the broader multimodal therapeutic approach in ADHD (Holtmann et al., 2014). Future research with larger samples, healthy controls, higher EEG resolution, and longer sleep recordings will help achieve more detailed and robust findings that could help prevent the neuropsychiatric consequences of the disorder.

Credit author statements

AF: Methodology, Software, Investigation, Data curation, Formal analysis, Writing - Original Draft, Visualization. CB: Methodology, Data curation, Conceptualization, Investigation, Writing - Original Draft. GM: Resources, Writing - Review & Editing. SDL: Investigation. PF: Formal analysis, Writing - Review & Editing. AM: Writing - Review & Editing, Supervision. EF: Writing - Review & Editing, Supervision. UF: Conceptualization, Resources, Writing - Review & Editing, Supervision. FS: Conceptualization, Resources, Writing - Review & Editing, Supervision, Project administration.

Declaration of competing interest

AF, CB, PF, AM, EF, FS report no potential conflict of interest. UF is co-founder and president of sleepActa S.r.l, a spin-off company of the University of Pisa operating in the field of sleep medicine. GM was in advisory boards for Angelini, received institutional research support from Angelini, Lundbeck and Humana, and was speaker for Angelini, Neuraxpharm and Otsuka.

Acknowledgments

This work has been partially supported by a grant from the IRCCS Fondazione Stella Maris (Ricerca Corrente 2020, and the "5 × 1000" voluntary contributions, Italian Ministry of Health). AF and EF have received funding from the European Union's Horizon 2020 Framework Programme for Research and Innovation under the Specific Grant Agreements No. 785907 (Human Brain Project SGA2) and No. 945539 (Human Brain Project SGA3). Authors thank Dr. Tommaso Banfi and Dr. Federico Cucchiara for their assistance with the code.

Appendix A. Supplementary data

Supplementary data to this article can be found online at https://doi.org/10.1016/j.jpsychires.2022.10.057.

References

Achenbach, T.M., 2001. Manual for ASEBA school-age forms & profiles. Univ. Vermont, Res. Cent. Child. Youth Fam.

Almeida Montes, L.G., Prado Alcántara, H., Martínez García, R.B., De La Torre, L.B., Ávila Acosta, D., Duarte, M.G., 2013. Brain cortical thickness in ADHD: age, sex, and clinical correlations. J. Atten. Disord. 17, 641–654. https://doi.org/10.1177/1087054711434351.

American Psychiatric Association, 2013. Diagnostic and Statistical Manual of Mental Disorders, fifth ed., DSM-5. American Psychiatric Association. https://doi.org/10.1176/appi.books.9780890425596.

Armitage, R., Emslie, G.J., Hoffmann, R.F., Rintelmann, J., Rush, A.J., 2001. Delta sleep EEG in depressed adolescent females and healthy controls. J. Affect. Disord. 63, 139–148. https://doi.org/10.1016/S0165-0327(00)00194-4.

Armitage, R., Hoffmann, R.F., Emslie, G.J., Weinberg, W.A., Mayes, T.L., Rush, A.J., 2002. Sleep microarchitecture as a predictor of recurrence in children and adolescents with depression. Int. J. Neuropsychopharmacol. 5, 217–228. https://doi.org/10.1017/S1461145702002948.

Banaschewski, T., Coghill, D., Zuddas, A., 2018. Oxford Textbook of Attention Deficit Hyperactivity Disorder.

Becker, S.P., 2020. ADHD and sleep: recent advances and future directions. Curr. Opin. Psychol. 34, 50–56. https://doi.org/10.1016/j.copsyc.2019.09.006.

Bernardi, G., Siclari, F., Yu, I., Zennig, C., Bellesi, M., Ricciardi, E., Cirelli, C., Ghilardi, M.F., Pietrini, P., Tononi, G., 2015. Neural and behavioral correlates of extended training during sleep deprivation in humans: evidence for local, task-

specific effects. J. Neurosci. 35, 4487–4500. https://doi.org/10.1523/JNEUROSCI.4567-14.2015.
Biancardi, C., Sesso, G., Masi, G., Faraguna, U., Sicca, F., 2021. Sleep EEG microstructure in children and adolescents with attention deficit hyperactivity disorder: a systematic review and meta-analysis. Sleep 1–14. https://doi.org/10.1093/sleep/zsab006.
Biederman, J., Monuteaux, M.C., Kendrick, E., Klein, K.L., Faraone, S.V., 2005. The CBCL as a screen for psychiatric comorbidity in paediatric patients with ADHD. Arch. Dis. Child. 90, 1010–1015. https://doi.org/10.1136/adc.2004.056937.
Biederman, J., Petty, C.R., Dolan, C., Hughes, S., Mick, E., Monuteaux, M.C., Faraone, S. V., 2008. The long-term longitudinal course of oppositional defiant disorder and conduct disorder in ADHD boys: findings from a controlled 10-year prospective longitudinal follow-up study. Psychol. Med. 38, 1027–1036. https://doi.org/10.1017/S0033291707002668.
Chang, L.Y., Wang, M.Y., Tsai, P.S., 2016. Diagnostic accuracy of Rating Scales for attention-deficit/hyperactivity disorder: a meta-analysis. Pediatrics 137. https://doi.org/10.1542/peds.2015-2749.
Cirelli, C., Tononi, G., 2019. Linking the need to sleep with synaptic function. Science 80. https://doi.org/10.1126/science.aay5304.
Conners Multi-Health Systems Inc, C.K., 2001. Conners' Rating Scales – Revised (CRS-R) : Technical Manual. Multi-Health Systems, North Tonawanda, N.Y.
Cortese, S., 2015. Sleep and ADHD: what we know and what we do not know. Sleep Med. 16, 5–6. https://doi.org/10.1016/j.sleep.2014.10.003.
Cucchiara, F., Frumento, P., Banfi, T., Sesso, G., Di Galante, M., D'Ascanio, P., Valvo, G., Sicca, F., Faraguna, U., 2020. Electrophysiological features of sleep in children with kir4.1 channel mutations and autism-epilepsy phenotype: a preliminary study. Sleep 43, 1–12. https://doi.org/10.1093/sleep/zsz255.
Delorme, A., Makeig, S., 2004. EEGLAB: an open source toolbox for analysis of single-trial EEG dynamics including independent component analysis. J. Neurosci. Methods 15, 9–21. Mar.
Delorme, A., Sejnowski, T., Makeig, S., 2007. Enhanced detection of artifacts in EEG data using higher-order statistics and independent component analysis. Neuroimage 34, 1443–1449. https://doi.org/10.1016/j.neuroimage.2006.11.004.
Donfrancesco, R., Miano, S., Martines, F., Ferrante, L., Melegari, M.G., Masi, G., 2011. Bipolar disorder co-morbidity in children with attention deficit hyperactivity disorder. Psychiatr. Res. 186, 333–337. https://doi.org/10.1016/j.psychres.2010.07.008.
Esser, S.K., Hill, S.L., Tononi, G., 2007. Sleep homeostasis and cortical synchronization: I. Modeling the effects of synaptic strength on sleep slow waves. Sleep 30, 1617–1630. https://doi.org/10.1093/sleep/30.12.1617.
Faraone, S.V., Asherson, P., Banaschewski, T., Biederman, J., Buitelaar, J.K., Ramos-Quiroga, J.A., Rohde, L.A., Sonuga-Barke, E.J.S., Tannock, R., Franke, B., 2015. Attention-deficit/hyperactivity disorder. Nat. Rev. Dis. Prim. 1 https://doi.org/10.1038/nrdp.2015.20.
Fauzan, N., Amran, N.H., 2015. Brain waves and connectivity of autism spectrum disorders. Procedia - Soc. Behav. Sci. 171, 882–890. https://doi.org/10.1016/j.sbspro.2015.01.204.
Feinberg, I., Campbell, I.G., 2013. Longitudinal sleep EEG trajectories indicate complex patterns of adolescent brain maturation. Am. J. Physiol. Regul. Integr. Comp. Physiol. 304, 296–303. https://doi.org/10.1152/ajpregu.00422.2012.
Ferrarelli, F., Kaskie, R., Laxminarayan, S., Ramakrishnan, S., Reifman, J., Germain, A., 2019. An increase in sleep slow waves predicts better working memory performance in healthy individuals. Neuroimage 191, 1–9. https://doi.org/10.1016/j.neuroimage.2019.02.020.
Franke, B., Michelini, G., Asherson, P., Banaschewski, T., Bilbow, A., Buitelaar, J.K., Cormand, B., Faraone, S.V., Ginsberg, Y., Haavik, J., Kuntsi, J., Larsson, H., Lesch, K. P., Ramos-Quiroga, J.A., Réthelyi, J.M., Ribases, M., Reif, A., 2018. Live fast, die young? A review on the developmental trajectories of ADHD across the lifespan. Eur. Neuropsychopharmacol 28, 1059–1088. https://doi.org/10.1016/j.euroneuro.2018.08.001.
Furrer, M., Jaramillo, V., Volk, C., Ringli, M., Aellen, R., Wehrle, F.M., Pugin, F., Kurth, S., Brandeis, D., Schmid, M., Jenni, O.G., Huber, R., 2019. Sleep EEG slow-wave activity in medicated and unmedicated children and adolescents with attention-deficit/hyperactivity disorder. Transl. Psychiatry 9. https://doi.org/10.1038/s41398-019-0659-3.
Goldstone, A., Willoughby, A.R., de Zambotti, M., Franzen, P.L., Kwon, D., Pohl, K.M., Pfefferbaum, A., Sullivan, E.V., Müller-Oehring, E.M., Prouty, D.E., Hasler, B.P., Clark, D.B., Colrain, I.M., Baker, F.C., 2018. The mediating role of cortical thickness and gray matter volume on sleep slow-wave activity during adolescence. Brain Struct. Funct. 223, 669–685. https://doi.org/10.1007/s00429-017-1509-9.
Gregory, A.M., Agnew-Blais, J.C., Matthews, T., Moffitt, T.E., Arseneault, L., 2017. ADHD and sleep quality: longitudinal analyses from childhood to early adulthood in a twin cohort. J. Clin. Child Adolesc. Psychol. 46, 284–294. https://doi.org/10.1080/15374416.2016.1183499.
Hanley, J.A., McNeil, B.J., 1982. The meaning and use of the area under a receiver operating characteristic (ROC) curve. Radiology 143, 29–36. https://doi.org/10.1148/radiology.143.1.7063747.
Holtmann, M., Sonuga-Barke, E., Cortese, S., Brandeis, D., 2014. Neurofeedback for ADHD: a review of current evidence. Child Adolesc. Psychiatr. Clin. N. Am. 23, 789–806. https://doi.org/10.1016/j.chc.2014.05.006.
Iber, C., Ancoli-Israel, S., Chesson, A.L., Quan, S.F., 2007. The AASM manual for the scoring of sleep and associated events: rules, terminology, and technical specifications. Am. Acad. Sleep Med.
Jaramillo, V., Volk, C., Maric, A., Furrer, M., Fattinger, S., Kurth, S., Lustenberger, C., Huber, R., 2020. Characterization of overnight slow-wave slope changes across development in an age-, amplitude-, and region-dependent manner. Sleep 43, 1–10. https://doi.org/10.1093/sleep/zsaa038.
Luo, Y., Weibman, D., Halperin, J.M., Li, X., 2019. A review of heterogeneity in attention deficit/hyperactivity disorder (ADHD). Front. Hum. Neurosci. 13, 1–12. https://doi.org/10.3389/fnhum.2019.00042.
Marangoni, C., De Chiara, L., Faedda, G.L., 2015. Bipolar disorder and ADHD: comorbidity and diagnostic distinctions. Curr. Psychiatr. Rep. 17, 1–9. https://doi.org/10.1007/s11920-015-0604-y.
Martiny, K., Nielsen, N.P., Wiig, E.H., 2020. Differentiating depression and ADHD without depression in adults with processing-speed measures. Acta Neuropsychiatr. https://doi.org/10.1017/neu.2020.17.
Masi, G., Mucci, M., Pfanner, C., Berloffa, S., Magazù, A., Perugi, G., 2012. Developmental pathways for different subtypes of early-onset bipolarity in youths. J. Clin. Psychiatr. 73, 1335–1341. https://doi.org/10.4088/JCP.11m07504.
Masi, G., Pietro, M., Azzurra, M., Simone, P., Annarita, M., 2015. Child behaviour checklist emotional dysregulation profiles in youth with disruptive behaviour disorders: clinical correlates and treatment implications. Psychiatr. Res. 225, 191–196. https://doi.org/10.1016/j.psychres.2014.11.019.
Massimini, M., Huber, R., Ferrarelli, F., Hill, S., Tononi, G., 2004. The sleep slow oscillation as a. Traveling Wave 24, 6862–6870. https://doi.org/10.1523/JNEUROSCI.1318-04.2004.
Mölle, M., Marshall, L., Gais, S., Born, J., 2002. Grouping of spindle activity during slow oscillations in human non-rapid eye movement sleep. J. Neurosci. Off. J. Soc. Neurosci. 22, 10941–10947. https://doi.org/10.1523/JNEUROSCI.22-24-10941.2002.
Nichols, T.E., Holmes, A.P., 2002. Nonparametric permutation tests for functional neuroimaging: a primer with examples. Hum. Brain Mapp. 15, 1–25. https://doi.org/10.1002/hbm.1058.
O'Neill, S., Rajendran, K., Mahbubani, S.M., Halperin, J.M., 2017. Preschool predictors of ADHD symptoms and impairment during childhood and adolescence. Curr. Psychiatr. Rep. 19 https://doi.org/10.1007/s11920-017-0853-z.
Plante, D.T., Goldstein, M.R., Cook, J.D., Smith, R., Riedner, B.A., Rumble, M.E., Jelenchick, L., Roth, A., Tononi, G., Benca, R.M., Peterson, M.J., 2016. Effects of partial sleep deprivation on slow waves during non-rapid eye movement sleep: a high density EEG investigation. Clin. Neurophysiol. 127, 1436–1444. https://doi.org/10.1016/j.clinph.2015.10.040.
Polanczyk, G., De Lima, M.S., Horta, B.L., Biederman, J., Rohde, L.A., 2007. The worldwide prevalence of ADHD: a systematic review and metaregression analysis. Am. J. Psychiatr. 164, 942–948. https://doi.org/10.1176/ajp.2007.164.6.942.
Prehn-Kristensen, A., Munz, M., Molzow, I., Wilhelm, I., Wiesner, C.D., Baving, L., 2013. Sleep promotes consolidation of emotional memory in healthy children but not in children with attention-deficit hyperactivity disorder. PLoS One 8. https://doi.org/10.1371/journal.pone.0065098.
Riedner, B.A., Vyazovskiy, V.V., Huber, R., Massimini, M., Esser, S., Murphy, M., Tononi, G., 2007. Sleep homeostasis and cortical synchronization: III. A high-density EEG study of sleep slow waves in humans. Sleep 30, 1643–1657. https://doi.org/10.1093/sleep/30.12.1643.
Ringli, M., Souissi, S., Kurth, S., Brandeis, D., Jenni, O.G., Huber, R., 2013. Topography of sleep slow wave activity in children with attention-deficit/hyperactivity disorder. Cortex 49, 340–347. https://doi.org/10.1016/j.cortex.2012.07.007.
Scarpelli, S., Gorgoni, M., D'Atri, A., Reda, F., De Gennaro, L., 2019. Advances in understanding the relationship between sleep and attention deficit-hyperactivity disorder (ADHD). J. Clin. Med. 8, 1737. https://doi.org/10.3390/jcm8101737.
Shaw, P., Eckstrand, K., Sharp, W., Blumenthal, J., Lerch, J.P., Greenstein, D., Clasen, L., Evans, A., Giedd, J., Rapoport, J.L., 2007. Attention-deficit/hyperactivity disorder is characterized by a delay in cortical maturation. Proc. Natl. Acad. Sci. U.S.A. 104 https://doi.org/10.1073/pnas.0707741104, 19649–19654.
Siclari, F., Bernardi, G., Riedner, B.A., LaRocque, J.J., Benca, R.M., Tononi, G., 2014. Two distinct synchronization processes in the transition to sleep: a high-density electroencephalographic study. Sleep 37, 1621–1637. https://doi.org/10.5665/sleep.4070.
Spiess, M., Bernardi, G., Kurth, S., Ringli, M., Wehrle, F.M., Jenni, O.G., Huber, R., Siclari, F., 2018. How do children fall asleep? A high-density EEG study of slow waves in the transition from wake to sleep. Neuroimage 178, 23–35. https://doi.org/10.1016/j.neuroimage.2018.05.024.
Steriade, M., Timofeev, I., Grenier, F., 2001. Natural Waking and Sleep States : A View from inside Neocortical Neurons 1969–1985.
Sung, V., Hiscock, H., Sciberras, E., Efron, D., 2008. Sleep problems in children with attention-deficit/hyperactivity disorder. Arch. Pediatr. Adolesc. Med. 162, 336. https://doi.org/10.1001/archpedi.162.4.336.
Thapar, A., Cooper, M., 2016. Attention deficit hyperactivity disorder. Lancet 387, 1240–1250. https://doi.org/10.1016/S0140-6736(15)00238-X.
Thorsen, A.L., Meza, J., Hinshaw, S., Lundervold, A.J., 2018. Processing speed mediates the longitudinal association between ADHD symptoms and preadolescent peer problems. Front. Psychol. 8, 1–9. https://doi.org/10.3389/fpsyg.2017.02154.

Tononi, G., Cirelli, C., 2014. Sleep and the price of plasticity: from synaptic and cellular homeostasis to memory consolidation and integration. Neuron 81, 12–34. https://doi.org/10.1016/j.neuron.2013.12.025.

Vyazovskiy, V.V., Riedner, B.A., Cirelli, C., Tononi, G., 2007. Sleep homeostasis and cortical synchronization: II. A local field potential study of sleep slow waves in the rat. Sleep 30, 1631–1642. https://doi.org/10.1093/sleep/30.12.1631.

Walg, M., Hapfelmeier, G., El-Wahsch, D., Prior, H., 2017. The faster internal clock in ADHD is related to lower processing speed: WISC-IV profile analyses and time estimation tasks facilitate the distinction between real ADHD and pseudo-ADHD. Eur. Child Adolesc. Psychiatr. 26, 1177–1186. https://doi.org/10.1007/s00787-017-0971-5.